2005

A Dynamin-3 Spliced Variant Modulates the Actin/Cortactin-Dependent Morphogenesis of Dendritic Spines

Noah W. Gray
Mayo Clinic

Anne E. Kruchten
Linfield College

Jing Chen
Mayo Clinic

Mark A. McNiven
Mayo Clinic

A dynamin-3 spliced variant modulates the actin/cortactin-dependent morphogenesis of dendritic spines

Noah W. Gray[1,*], Anne E. Kruchten[2], Jing Chen[2] and Mark A. McNiven[1,2,‡]

[1]Molecular Neuroscience Program and Graduate School, Mayo Clinic, Rochester, MN 55905, USA
[2]Department of Biochemistry and Molecular Biology, Mayo Clinic, Rochester, MN 55905, USA
*Present address: Howard Hughes Medical Institute, Cold Spring Harbor Laboratory, 1 Bungtown Road, Cold Spring Harbor, NY 11724, USA
‡Author for correspondence (e-mail: mmcniven@mayo.edu)

Accepted 7 January 2005
Journal of Cell Science 118, 1279-1290 Published by The Company of Biologists 2005
doi:10.1242/jcs.01711

Summary

Immature dendrites extend many actin-rich filopodial structures that can be replaced by synapse-containing dendritic spines as the neuron matures. The large GTPase dynamin-3 (Dyn3) is a component of the postsynapse in hippocampal neurons but its function is undefined. Here, we demonstrate that a specific Dyn3 variant (Dyn3baa) promotes the formation of immature dendritic filopodia in cultured neurons. This effect is dependent upon Dyn3 GTPase activity and a direct interaction with the F-actin-binding protein cortactin. Consistent with these findings, Dyn3baa binds to cortactin with a 200% higher affinity than Dyn3aaa, a near identical isoform that does not induce dendritic filopodia when expressed in cultured neurons. Finally, levels of Dyn3baa-encoding mRNA are tightly regulated during neuronal maturation and are markedly upregulated during synaptogenesis. Together, these findings provide the first evidence that an enhanced interaction between a specific Dyn3 splice variant and cortactin modulate actin-membrane dynamics in developing neurons to regulate the morphogenesis of dendritic spines.

Supplementary material available online at
http://jcs.biologists.org/cgi/content/full/118/6/1279/DC1

Key words: Dynamin, Cortactin, Filopodia, Actin, Neuron

Introduction

Synaptogenesis is initiated by the dynamic activities of axons and growth cones, as well as by dendrites and dendritic protrusions (Jontes and Smith, 2000). During the development of cultured hippocampal neuron, synaptogenesis generally occurs between 6 and 14 days in vitro (DIV), with most dendritic protrusions maintaining a filopodial morphology (Dailey and Smith, 1996; Ziv and Smith, 1996). These filopodia are long, thin, actin-rich structures with or without an enlargement of the tip (Hering and Sheng, 2001). As these neurons and synapses mature, the immature filopodia are replaced by shorter, mature mushroom-shaped dendritic spines containing the postsynaptic density (Fiala et al., 1998; Papa et al., 1995).

The general morphological profile and dynamics of filopodia and dendritic spines have been previously described (Hering and Sheng, 2001), although little is known about the molecular mechanisms underlying the morphological conversion of filopodia to mature, mushroom-shaped spines. The dynamin family of large GTPases are potential candidates to participate in this important process, because they are believed to provide a dynamic link between cell membranes and the actin cytoskeleton via a pleckstrin homology (PH) domain and a proline/arginine-rich domain (PRD), respectively (Orth and McNiven, 2003; Schafer, 2002). Three conventional dynamin isoforms are expressed in neurons. Dyn1 is neuron specific (Nakata et al., 1991) and is found primarily in the presynapse (Gray et al., 2003), where it is required for synaptic-membrane endocytosis and recycling (Shupliakov et al., 1997; Takei et al., 1996). Dyn2 is expressed in all tissues (Cook et al., 1994; Sontag et al., 1994) and participates in a range of endocytic and secretory membrane-trafficking events. By contrast, little is known about the expression, cellular distribution and function of Dyn3. This poorly understood form exhibits some tissue-specific expression and is found primarily in the brain, lung and testis (Cook et al., 1996; Nakata et al., 1993).

In a previous study, we presented evidence suggesting that Dyn3 accumulated at the postsynapse and localized to dendritic spines and filopodia (Gray et al., 2003). There are two expressed spliceoforms of Dyn3, Dyn3aaa and Dyn3baa, which differ by only ten amino acids spliced into Dyn3baa immediately preceding the PH domain (Cao et al., 1998). Both spliceoforms were expressed in hippocampal neurons to test whether these proteins contributed to G-protein-coupled-receptor endocytosis at the synapse. Although Dyn3 did not appear to contribute to the endocytic recycling of the metabotropic glutamate receptor, we did observe a striking change in the morphology of mature neurons expressing a fusion between Dyn3baa and green fluorescent protein (GFP) (Gray et al., 2003), a phenotype that suggested a postsynaptic function. Specifically, these transfected neurons lacked mature dendritic spines and were covered instead by long, thin filopodia.

In the current study, we observe that early and constitutive

expression of Dyn3baa, but not Dyn3aaa, leads to an aberrant maturation of dendritic spines and a reduction in filopodia and spine synapses. This phenotype is dependent upon an intact actin cytoskeleton and the GTPase activity of Dyn3baa. Remarkably, filopodia can also be induced in epithelial cells that do not normally express Dyn3. To define how Dyn3baa might produce these changes, we tested for functional and physical interactions between Dyn3 and the actin bundling protein cortactin, which is also a known structural component of the postsynapse (Hering and Sheng, 2003; Naisbitt et al., 1999). Cortactin and Dyn2 are known to bind directly (McNiven et al., 2000) and disruption of this interaction has been shown to have profound effects on actin-based structures within cells, such as stress fibers (McNiven et al., 2000), actin comets (Lee and De Camilli, 2002; Orth et al., 2002) and dorsal ruffles (Krueger et al., 2003). Importantly, reducing Dyn3-cortactin interactions in cultured neurons through the expression of C-terminally truncated proteins prevents the observed aberrant neuronal filopodial outgrowth. In support of this in vivo observation, we find that, although both Dyn3 spliceoforms can bind to cortactin directly, the filopodium-inducing Dyn3baa exhibits a twofold greater affinity for cortactin than does Dyn3aaa, the form that allows the normal development of mature, mushroom-shaped dendritic spines. In support of these different effects, we also observe markedly distinct expression patterns of the two Dyn3 spliceoforms during synaptogenesis and filopodium and spine maturation. This study provides the first functional insights for Dyn3 in any cell type or tissue and is consistent with a novel developmental role for this dynamin family member in spine synaptogenesis. We also discuss the contributions of Dyn3 to actin-based membrane dynamics during synaptic remodeling.

Materials and Methods

Plasmid construction and transfection

Dyn3aaa-GFP and Dyn3baa-GFP were produced as described (Gray et al., 2003), and Dyn3baa(K44A)-GFP was produced using the Quikchange site-directed mutagenesis kit (Stratagene). Mutants of Dyn3aaa and Dyn3baa with the PRDs deleted (Dyn3aaaΔPRD and Dyn3baaΔPRD) were produced by amplifying a Dyn3 fragment from the full-length GFP-tagged plasmids using primers designed to remove the C-terminal 115 amino acids of each spliced variant. The resulting PCR product was cloned into the pEGFP-C_1 vector (Clontech). A fusion between cortactin and red fluorescent protein (cortactin-RFP) and a mutant of this with the SH3 domain deleted (cortactinΔSH3-RFP) were produced as previously described (Cao et al., 2003). Fusions between Dyn3aaa and Dyn3baa, and glutathione-*S*-transferase (Dyn3aaa-GST and Dyn3baa-GST) were produced by PCR amplification of each spliced variant from the GFP-tagged plasmids, including the reintroduction of a stop codon. These Dyn3 products were cloned into the pGEX-3X vector (Amersham). For His_6-tagged protein, full-length cortactin was PCR amplified from GFP-tagged plasmids, with the reintroduction of a stop codon, and cloned into the pQE80 vector (Qiagen).

Cultures and transfection

Hippocampal neuronal cultures from Sprague-Dawley rats at embryonic day 18 (E18) were prepared as previously described (Gray et al., 2003). Neurons were fed twice weekly by changing half of the medium. Neuronal cultures were transfected at 6DIV using endotoxin-free DNA with Effectene (Qiagen) according to the manufacturer's protocol. For co-transfections, equal amounts of empty cyan fluorescent protein (CFP) vector (Clontech) and each GFP construct or equal amounts of Dyn3-GFP and cortactin-RFP were used in the same transfection reaction. Neurons were used 5-12 days after transfection. In all cases, transfection-complex-containing medium was exchanged after a 4 hour incubation with the cells.

COS-7 cells were grown in DMEM + 10% fetal calf serum and antibiotics. Cells were transfected with Effectene as described above and used 48 hours later. All cell-culture reagents were from Invitrogen.

Quantitation of spine/filopodium phenotypes and immunofluorescence

Neurons were transfected with the following combinations: GFP and CFP empty vectors; Dyn3aaa-GFP and CFP; Dyn3baa-GFP and CFP; or Dyn3baa(K44A)-GFP and CFP. The neurons were then fixed and processed as previously described (Gray et al., 2003). Once a transfected cell was identified by epifluorescence, it was imaged using a Zeiss LSM 510 confocal microscope equipped with a Zeiss 63× objective (1.4 NA) and an argon/krypton laser set to a wavelength of 428 nm to excite only the CFP fluorophore. All measurements of dendritic length, filopodium/spine length and protrusion density were completed using IPLab software (Scanalytics). Spine heads were identified when the tip of a dendritic protrusion was 2 pixels larger than the shaft. For quantitation of synaptic contacts, Dyn3aaa-GFP- or Dyn3baa-GFP-expressing cells were immunolabeled with either PSD-95 (Affinity Bioreagents) or synapsin (gift of P. McPherson, McGill University) antibodies and imaged using a cooled CCD camera (Hamamatsu Photonics). Images were prepared for quantitation using Adobe Photoshop. Blinded observers completed all quantitation. For each transfection condition, spine length, density and spine head presence were determined from 15-20 cells, analysing 4-6 mm total measured dendritic length and 3000-5000 spines/filopodia in total. Quantitation of the proportion of spines containing PSD-95 or adjacent to synapsin was completed on 15-20 cells from each transfection condition in which 1000-1200 spines/filopodia in total were examined. A spine/filopodium was scored as possessing synaptic machinery if it either contained PSD-95 clusters or was directly adjacent to synapsin. For statistical analysis, analysis of variance (ANOVA) and Fisher's protected-least-significant-difference (PLSD) tests were completed using StatView (SAS Institute). To test for actin sensitivity, neurons were treated with 1 μM latrunculin A (LatA) (Molecular Probes) or an equivalent volume of dimethylsulfoxide (DMSO) for 18 hours before fixation and staining with rhodamine-phalloidin (Sigma). To test for the localization of active synapses, uptake assays for the styryl dye N-(3-triethylammoniumpropyl)-4-{6-[4-(diethylamino)phenyl]hexatrienyl} pyridinium dibromide (FM4-64) were completed at 18DIV on transfected neurons. Neurons were pre-equilibrated in Tyrode's solution [composed of (in mM) 145 NaCl, 5.4 KCl, 1.8 $CaCl_2$, 0.8 $MgCl_2$, 10 Hepes and 10 glucose (pH 7.4, osmolarity 310 mOsm)] followed by 30 seconds of depolarization in Tyrode's solution adjusted to 90 mM KCl. Depolarization solution contained glutamate-receptor blockers [100 μM 2-amino-5-phosphonopentanoate (AP-5) and 20 μM 6,7-dinitroquinoxaline-2,3-dione (DNQX)] and 15 μM FM4-64. Cultures were washed with regular Tyrode's solution containing glutamate-receptor blockers for 10 minutes, fixed and imaged immediately.

RNA isolation and RT-PCR

Three time-course sample collections were completed from three separate neuronal isolations. In addition, hippocampal tissues were collected from Sprague-Dawley rats (pooled from three different individuals) at various time points throughout development. For reverse-transcription PCR (RT-PCR), total RNA was isolated from either the neuronal cultures or the hippocampal tissue at each time point and used to make a cDNA library as previously described (Cao

et al., 1998). Neurons were cultured as described above, except that cells were grown in poly-L-lysine-coated plastic dishes instead of on coverslips. Reactions were carried out as previously described (Cao et al., 1998). Primers were designed to flank the 30-nucleotide splicing region within the mid/PH domain of Dyn3; sequences were 5′-ACGTCCCGGACTTTCAGG-3′ and 5′-ACTTCCCCAGACTTTG-TG-3′, producing products of 370 bp (Dyn3aaa) and 400 bp (Dyn3baa), small fragments of the entire transcript. Total levels of *Dyn3* mRNA were determined using primers that were previously described (Cao et al., 1998). Glyceraldehyde-3-phosphate dehydrogenase (GAPDH) was detected with primers as previously described (Gray et al., 2003). In order to visualize multiple Dyn3 spliced variants, samples were separated on a 3% agarose gel and post-stained with ethidium bromide.

Direct binding assays

100-200 nM GST, Dyn3aaa or Dyn3baa was combined with 200 nM His_6-tagged recombinant cortactin and glutathione-Sepharose beads (Sigma) in immunoprecipitation (IP) buffer for 1 hour at 4°C. After several washes with IP buffer, complexes were boiled and eluted in 2× Laemmli sample buffer and separated on 10% SDS-PAGE gels. Proteins were transferred to PVDF membrane and western blots were performed using a mouse RGS-His_6 antibody at 1:1000 (Qiagen) as previously described (Gray et al., 2003).

To determine the different binding dynamics of Dyn3aaa and Dyn3baa to cortactin, a blot-overlay method was used. Various amounts (3-500 ng) of recombinant Dyn3 proteins were spotted onto Nitrobind nitrocellulose transfer membrane (Micron Separations) using a Minifold II Slot Blotter (Schleicher & Schueller). After spotting, the membrane was blocked in 10% milk in PBS for 1 hour at room temperature. The membrane was then incubated in a cortactin overlay solution at 50 μg ml^{-1} for 1 hour at room temperature. The membrane was washed in PBS+0.05% Tween-20 (PBST) and then incubated with anti-cortactin antibody for 1 hour. Subsequent steps were completed for western blotting as described above. A control experiment excluding the cortactin overlay and blotting with anti-dynamin antibodies was performed to assess equal spotting of dynamin protein. Quantitation was performed using Bio-Rad densitometry software to measure band intensity as a readout of Dyn3-cortactin binding. Results were averaged from three independent experiments. Resulting data were normalized to the maximum intensity and plotted on a scale from 0 to 1. This allowed for comparisons across experiments. Fold differences in binding were calculated by dividing densitometry measurements for Dyn3baa bands by measurements for Dyn3aaa bands and averaging the fold differences over three experiments. Errors were expressed as standard error of the mean.

Theoretical modeling

Molecular models of the Dyn3baa sequence were generated to produce a theoretical visual interpretation of the insert and its possible effects on protein structure. Sequences from the region surrounding the insert of Dyn3baa and Dyn3aaa proteins (residues 484-652 or 484-642, respectively) were aligned against the sequence for the pleckstrin homology (PH) domain of Rac. Alignment was achieved using the T-Coffee multiple sequence alignment server (http://igs-server.cnrs-mrs.fr/Tcoffee/tcoffee-cgi/index.cgi) (Notredame et al., 2000; Poirot et al., 2004). Alignment sequences were submitted to the Alignment Interface of the SWISS-MODEL Automated Protein Modeling Server (http://swissmodel.expasy.org//SWISS-MODEL.html) (Guex and Peitsch, 1997; Peitsch, 1995; Schwede et al., 2003) and modeled against the known crystal coordinates of the Rac PH domain. Coordinate files results were received by email from SWISS MODEL and visualized using RasMac (RasMac Molecular Graphics). Although the crystal structure of the PH domain of dynamin has been solved, the Dyn3baa insert extends beyond the known crystallized sequence and therefore could not be used for molecular modeling of the Dyn3baa insert region. Alignments generated against PH domains of Grp1 and Akt also produced results indicating the insert region of Dyn3baa folds into an extended turn region.

Results

Dyn3baa induces filopodial outgrowth in mature neurons

We have previously observed that the expression of Dyn3baa-GFP induced a marked outgrowth of filopodia from transfected cells and a marked decrease in the normal distribution of mushroom-shaped dendritic spines (Gray et al., 2003) (Fig. 1B). This surprising finding provided a functional correlate to support our biochemical and

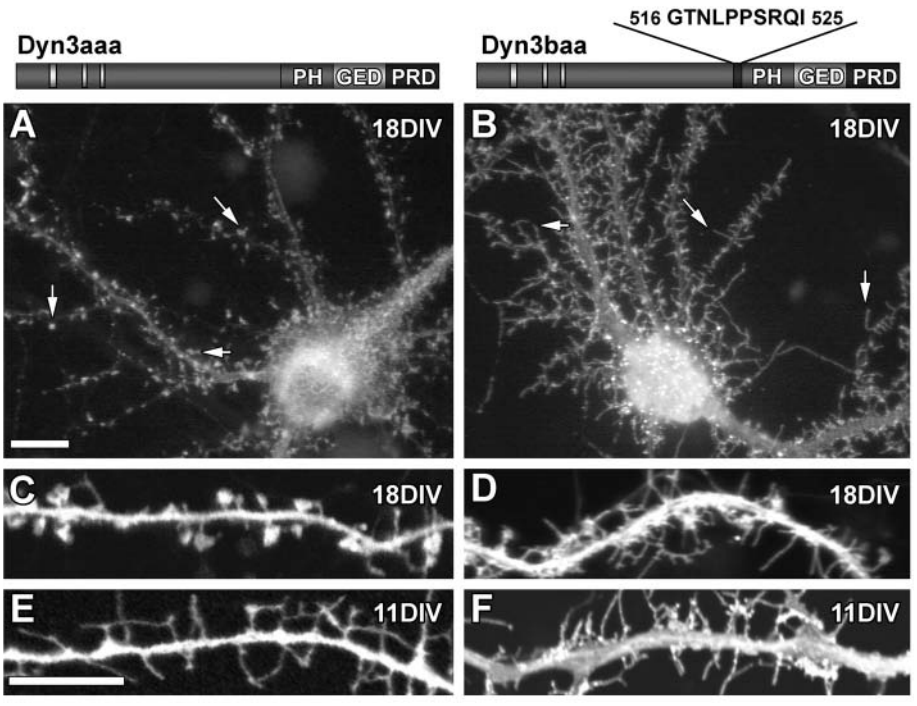

Fig. 1. The expression of distinct Dyn3 variants induces profoundly different postsynaptic morphologies. (A,C) Neurons transfected with Dyn3aaa-GFP produce numerous mushroom-shaped dendritic spines by 18DIV (arrows in A). (B,D) Neurons expressing Dyn3baa-GFP exhibit morphologically immature dendritic spines at a mature culture age, with long filopodia remaining as the dominant structures instead of spines (arrows in B). (E,F) Although Dyn3aaa- and Dyn3baa-expressing neurons appear different at 18DIV, they exhibit remarkably similar morphologies at 11DIV, when filopodia normally persist. Images in C-F represent CFP fluorescence from Dyn3-spliceoform-co-transfected cells captured by confocal microscopy. Scale bars, 5 μm.

Table 1. Quantitation of spine/filopodium morphology from transfected neurons

	GFP	Dyn3aaa	Dyn3baa	Dyn3baa KA
11 DIV				
Mean number of spines per 10 μm of dendrite	6.4±0.9	5.5±1.0	5.6±1.2	5.5±1.0
Mean overall spine length (μm)	1.5±0.2	1.8±0.3	2.0±0.2	1.3±0.2
Number of spines >2 μm long per 100 μm of dendrite	13.5±4.3	16.9±4.7	20.3±5.0	**6.1±2.6**
Proportion of spines with heads (%)	14.9±4.2	21.4±8.5	13.0±4.2	**55.3±8.7**
18 DIV				
Mean number of spines per 10 μm of dendrite	6.0±0.7	5.7±0.8	**8.9±1.4**	5.3±1.3
Mean overall spine length (μm)	0.9±0.1	1.1±0.1	1.4±0.1	1.2±0.2
Number of spines >2 μm long per 100 μm of dendrite	2.5±2.1	2.6±1.9	**16.6±4.1**	5.5±2.4
Proportion of spines with heads (%)	76.9±10.3	77.6±9.5	**29.1±6.8**	69.3±9.8

All values are expressed as the mean±s.d.

Bold numbers indicate a significant statistical difference ($P<0.001$) between that transfection condition and all other transfection conditions within each specific measurement. ANOVAs followed by Fisher's PLSD test were performed for each measurement.

morphological observations, suggesting that a population of Dyn3 is a component of the postsynapse. This prominent phenotype was apparent 2-3 days following transfection and persisted for the life of the neuron (up to 4 weeks in culture), but was not observed in neurons expressing Dyn3aaa (Fig. 1A). The maintenance of the filopodia induced by Dyn3baa expression was actin dependent, because treatment with 1 μM LatA (a sponge metabolite that causes the depolymerization of actin filaments) resulted in a complete loss of these filopodia and an accumulation of Dyn3baa-GFP clusters throughout the dendritic shafts (see Fig. S1 in supplementary material). The same treatment with vehicle alone (DMSO) had no effect on the spine/filopodium morphology. Because it is known that immature neurons normally extend numerous filopodia that are gradually replaced by mature spines (Papa et al., 1995), we compared transfected neurons at two different ages for a rigorous quantitation of this Dyn3baa-expression phenotype. Neurons were co-transfected at 5-6DIV with empty CFP vector (in order to volumetrically fill and label all neuronal processes/protrusions) and with GFP vector, Dyn3aaa-GFP or Dyn3baa-GFP. Transfected cultures were then analysed at 11DIV, at which time endogenous dendritic filopodia are immature and abundant, and at 18DIV, when synaptogenesis has reached an equilibrium and dendritic spines are the dominant excitatory postsynaptic structure. Upon a positive identification of neuronal GFP construct expression, the dendrites were imaged by confocal microscopy to excite and visualize only the CFP fluorescence. This strategy allowed the capture of dendritic images in which the fluorescent signal was uniformly distributed throughout the physical structure of the neuron under all transfection conditions, making quantitative measurements more accurate. On average, mature dendritic spines in cultured neurons are 0.8-1.0 μm in length and exhibit an enlarged spine head (El-Husseini et al., 2000). Filopodia can vary in length (up to 5 μm) and usually lack this distal swelling (Papa et al., 1995). The length and density of the spines in mature control cultures (GFP alone) were similar in value to those that have been previously reported in both dissociated neurons and in brain tissue (El-Husseini et al., 2000; Sorra and Harris, 2000) (Table 1).

Neurons expressing Dyn3aaa-GFP possessed numerous filopodia without heads at 11DIV (Fig. 1E) but, at 18DIV, most of these had been replaced by shorter, mushroom-shaped spines (Fig. 1C). These same observations were made in neurons expressing GFP vector (data not shown). Neurons expressing Dyn3baa-GFP appeared to be similar to Dyn3aaa-GFP-expressing neurons at 11DIV, possessing numerous filopodia (Fig. 1F). Interestingly, at the mature stages of development (18DIV), these Dyn3baa-expressing neurons maintained mostly filopodia, and most transfected neurons lacked mushroom-shaped spines (Fig. 1D). Quantification of the differences in dendritic protrusion morphology between neurons expressing each Dyn3 spliceoform used two main criteria to distinguish immature filopodia and mature dendritic spines: spine/filopodium length and the presence or absence of a spine head or distal enlargement of the dendritic protrusion. After quantifying the morphological profile of protrusions for each transfection condition, we found that there were no differences in the density of long dendritic protrusions (>2 μm; Fig. 2A, Table 1) or in the proportion of dendritic protrusions that contained an enlarged head (Fig. 2B, Table 1) for neurons expressing GFP, Dyn3aaa-GFP, or Dyn3baa-GFP analysed at 11DIV. Conversely, at 18DIV, although morphological quantitation of neurons expressing Dyn3aaa-GFP and GFP alone revealed overlapping phenotypes, our results from neurons expressing Dyn3baa-GFP were significantly different (Fig. 2A,B, Table 1). The quantitation for Dyn3baa-GFP-expressing neurons at 18DIV were similar to the results acquired at 11DIV, suggesting that these cells had maintained this filopodium-rich phenotype and were perhaps 'locked' in a more immature state, implicating Dyn3 in the regulation of spine maturation. We also tested a GTPase-defective Dyn3baa mutant to test whether this filopodial gain-of-function phenotype depended upon the GTPase activity of Dyn3baa (see below).

Dyn3baa-induced filopodia do not undergo mature synaptic assembly

To use a more functional criterion in the determination of dendritic spine/filopodial age, we next sought to explore whether synaptogenesis was affected in cells expressing Dyn3baa. We analysed the synaptic network in cultures transfected with GFP vector, Dyn3aaa-GFP or Dyn3baa-GFP by labeling for both postsynaptic and presynaptic markers (PSD-95 and synapsin, respectively), and then quantified the number of synaptic puncta in transfected cells that localized with dendritic protrusions. At 11DIV, less than 25% of filopodia were associated with either synaptic marker under

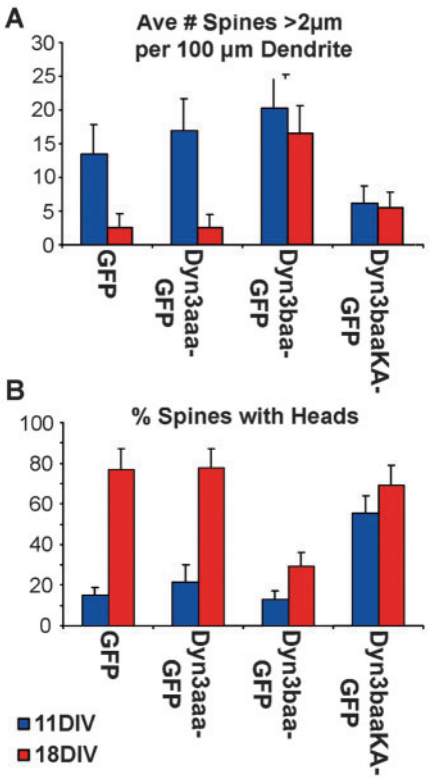

Fig. 2. Dyn3baa inhibits the development of normal neuronal morphology. Neuron morphology was quantified using two morphological criteria to distinguish between filopodia and spines. 18DIV Dyn3baa-expressing cells remained similar to 11DIV cultures with respect to protrusion length (A) and presence of a spine head (B), indicating that filopodia at 11DIV do not mature into spines by 18DIV in these neurons. By contrast, control neurons expressing Dyn3aaa-GFP or GFP exhibit this normal progression during development from filopodia to spines. Expression of the GTPase-deficient Dyn3baaKA-GFP did not affect the morphology of transfected neurons at 18DIV but did cause immature (11DIV) transfected neurons to contain morphologically mature spines. All error bars represent s.d.

any transfection conditions (Fig. 3E,F). Conversely, at 18DIV, 75-80% of protrusions from cells transfected with GFP or Dyn3aaa-GFP were associated with synaptic markers (Fig. 3E,F). At 18DIV, Dyn3aaa-GFP was found in spine heads, where it was juxtaposed to the presynaptic sites (labeled with synapsin) of untransfected neurons (Fig. 3A, arrows) and localized with PSD-95 (Fig. 3C, arrows). These synaptic puncta were also determined to be active synapses by using the styryl dye FM4-64 to label sites of rapid endocytosis following high K^+ depolarization, and most spines from these older cultures were juxtaposed to FM4-64-positive puncta (see Fig. S2 in supplementary material). At 18DIV, dendritic protrusions found on neurons transfected with Dyn3baa-GFP were rarely juxtaposed to synapsin-positive presynaptic terminals (Fig. 3B, arrows) and most did not contain PSD-95 clusters (Fig. 3D, arrows). Our quantitation confirmed these trends, with filopodia/spines from 18DIV Dyn3baa-GFP-expressing neurons exhibiting a similar association with synaptic markers as 11DIV neurons (Fig. 3E,F). Also, filopodia from Dyn3baa-GFP neurons did not associate with FM4-64-positive puncta, although some dye accumulation was observed along the dendritic shafts of Dyn3baa-expressing neurons (see Fig. S2 in supplementary material). Taken together, these morphological observations indicated that synaptogenesis onto dendritic protrusions is significantly reduced in neurons expressing Dyn3baa-GFP.

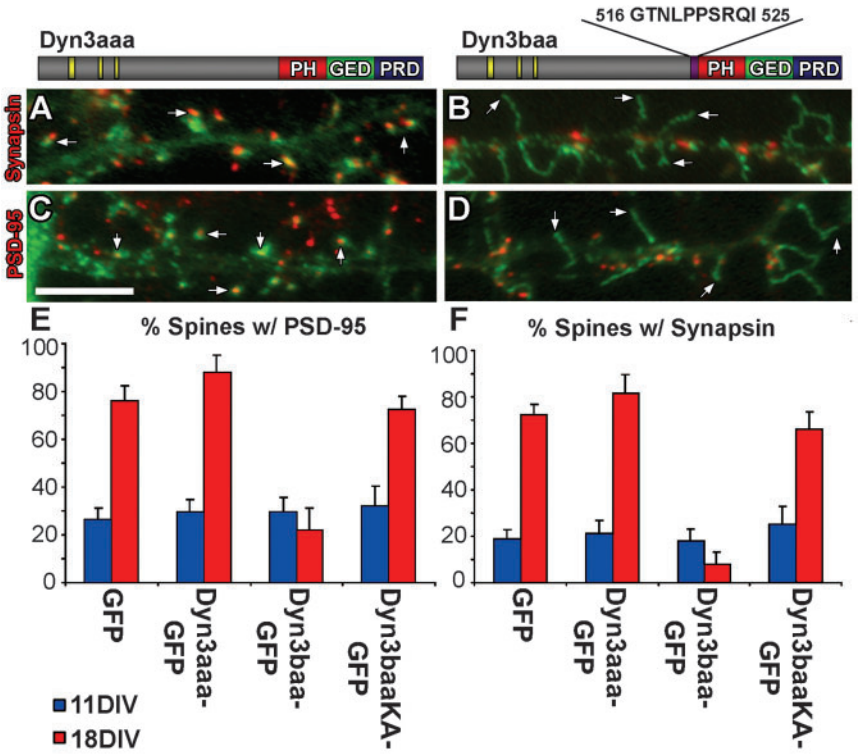

Fig. 3. Synaptogenesis is impaired in Dyn3baa-expressing neurons. Neurons transfected with Dyn3aaa-GFP (A,C) or Dyn3baa-GFP (B,D) at 18DIV were labeled for the presynaptic marker synapsin (A,B) or the postsynaptic marker PSD-95 (C,D). Dyn3aaa-GFP was found to be directly juxtaposed to synapsin-positive puncta (arrows in A) and colocalized with PSD-95 (arrows in C). Dyn3baa-GFP and dendritic filopodia were neither directly juxtaposed to synapsin-positive puncta (arrows in B) nor colocalized with PSD-95 (arrows in D). (E,F) Quantitation of association between dendritic protrusions and synaptic markers revealed that control neurons exhibited little association with synaptic markers at 11DIV but extensive association at 18DIV. By contrast, neurons transfected with Dyn3baa-GFP exhibited impaired dendritic spine synaptogenesis, with 20% of filopodia containing PSD-95 (E) and less than 10% of filopodia juxtaposed to synapsin (F) at 18DIV. Neurons expressing a GTPase-deficient mutant Dyn3baa-GFP (KA mutant) did not exhibit this maturation defect and progressed normally through synaptogenesis with culture age. All error bars represent s.d. Scale bar, 5 µm.

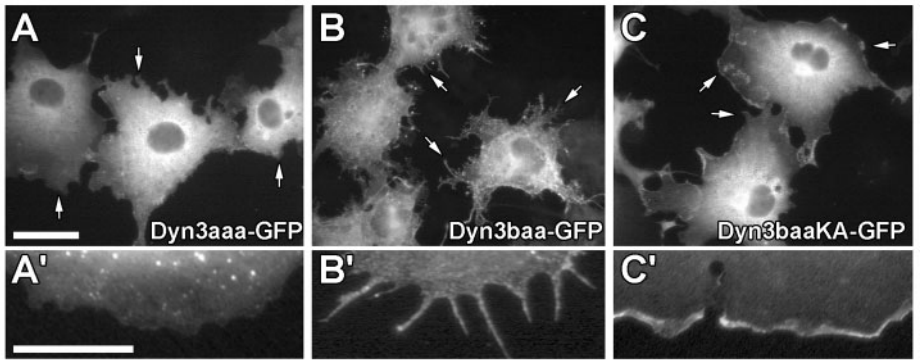

Fig. 4. Dyn3baa-GFP induces filopodial outgrowth in non-neuronal cells. COS-7 cells transfected with Dyn3aaa-GFP (A) maintained a normal morphology, with a smooth lamellar perimeter (arrows in A, close-up in A′) and a rounded shape. By contrast, COS-7 cells transfected with Dyn3baa-GFP exhibited radical shape changes (B), with the smooth perimeter often replaced with numerous large membranous protrusions and long filopodia that were remarkably similar to the filopodia in neurons (arrows in B, close-up in B′). Transfection with Dyn3baa(KA)-GFP caused a phenotype resembling Dyn3aaa-GFP transfection, causing cells to maintain their normal smooth perimeter (C). Interestingly, mutant Dyn3baa remained at the membrane perimeter (arrows in C, close-up in C′) but did not induce the shape changes observed with Dyn3baa wild-type transfection. Scale bar, 10 μm.

Dyn3baa induces filopodia in a heterologous system

To test whether Dyn3baa-induced filopodium formation was a conserved function and not an expression artefact specifically in neurons, we expressed Dyn3baa-GFP in COS-7 cells, a cell type that is normally discoidal in shape, does not abundantly produce filopodia and does not endogenously express Dyn3. COS-7 cells expressing Dyn3aaa-GFP maintained a characteristically smooth plasma-membrane perimeter, lacking numerous filopodia (Fig. 4A,A′). By dramatic contrast, cells expressing Dyn3baa-GFP were uniquely shaped, with numerous small membranous protrusions and rows of filopodia (Fig. 4B,B′). Nearly all transfected cells lost their normal smooth, rounded appearance and adopted a more spindly and spiky shape. Based on these data in COS-7 cells, this filopodium-inducing function for Dyn3baa is not peculiar to neurons, with Dyn3baa seeming to perform an important role in the machinery that produces and maintains filopodia in cells.

Dyn3baa GTPase activity is required for filopodium formation

To test whether the enzymatic activity of Dyn3baa was necessary for the induction and/or maintenance of dendritic filopodia, a GTPase-deficient Dyn3baa was constructed containing a mutation (K44A) in the highly conserved GTPase region of the protein (Damke et al., 1994). Surprisingly, Dyn3baa(K44A)-GFP overexpression produced a normal morphological phenotype in neurons at 18DIV, with these cells displaying short, mushroom-shaped spines (Fig. 2A,B, Table 1). Interestingly, based on our quantitation at 11DIV, neurons transfected with the GTPase-defective Dyn3baa(K44A)-GFP developed mature morphological characteristics at this earlier time, making these 11DIV neurons more similar to mature 18DIV neurons, the opposite effect to wild-type-Dyn3baa/GFP expression. Although this morphological difference at 11DIV was observed in cells expressing the Dyn3baa mutant, no effect on spine/filopodium synaptogenesis was observed (Fig. 3E,F). Taken together, these results suggest that GTPase-deficient Dyn3baa might actually enhance or facilitate the morphological development of dendritic spines but has no effect on spine synapse assembly.

In parallel studies with cultured epithelial cells, GTPase-dead Dyn3baa did not induce filopodia in this heterologous system (Fig. 4C,C′), consistent with the notion that the wild-type enzymatic activity is important during the reorganization of the cell periphery. Interestingly, although filopodia were not induced in these Dyn3baa-mutant-expressing cells, the exogenous protein was recruited to the membrane perimeter in putative lamellipodia (Fig. 4C, arrows), even incorporating into what appeared to be membrane ruffles. By contrast, Dyn3aaa-GFP seldom extended all the way out to the plasma membrane of the COS-7 cells (Fig. 4A′). This suggests that, in both epithelial and neuronal cell types, the targeting of Dyn3baa does not require enzymatic activity but the formation of discrete filopodia does.

Dyn3 spliced variants bind differently to cortactin

Previously, the PRD of Dyn2 was found to bind to the SH3 domain of the actin-binding protein cortactin (McNiven et al., 2000). Interestingly, the region of the Dyn2 PRD that mediates this interaction is nearly identical in Dyn3 (Fig. 5A). To test whether Dyn3 and cortactin also bind, we performed immunoprecipitation experiments using Dyn3-GST and His_6-cortactin. Although GST alone did not pull down cortactin, both Dyn3 spliceoforms isolated cortactin, confirming a direct interaction between these two proteins (Fig. 5B). This novel link to the actin cytoskeleton for Dyn3 is interesting considering the actin dependence of the Dyn3baa-induced filopodia and the fact that cortactin is a prominent component of the post-synapse (Hering and Sheng, 2003; Naisbitt et al., 1999).

Because these initial cortactin-Dyn3 immunoprecipitation-based binding experiments were largely qualitative and we wanted to gain insight into how this direct interaction might contribute to spine formation, we next tested for different binding affinities for the two Dyn3 spliceoforms to cortactin using quantitative blot-overlay experiments. In each case, 3-500 ng of each Dyn3 spliced variant was spotted onto membranes followed by an overlay with an excess of recombinant cortactin. The cortactin was detected with antibodies, and binding was quantified using a densitometer (Fig. 5C). A control experiment using antibodies against Dyn3 was performed and quantified by densitometry to assure even spotting of dynamin protein (data not shown). Signals were normalized to the maximum intensity so that comparisons could be made across experiments. Binding curves were generated from the densitometry data (Fig. 5D) and the steeper slope and higher maximum intensity of the Dyn3baa curve

demonstrated its stronger affinity for cortactin than that of Dyn3aaa. Differences in binding were also calculated, showing at least a twofold increase in cortactin binding for Dyn3baa over Dyn3aaa at all tested concentrations (Fig. 5E). The larger binding variations at lower cortactin concentrations are most likely due to the spotting of small protein quantities and film inconsistencies. The difference in cortactin affinity between Dyn3aaa and Dyn3baa was significant ($P<0.05$ for 300 ng and 500 ng) and reflected three separate experiments. Thus, although the PRDs of both Dyn3aaa and Dyn3baa are identical, the insert present in Dyn3baa is likely to impose certain structural modifications on the rest of the C-terminal region of the protein, which results in a markedly increased affinity for cortactin.

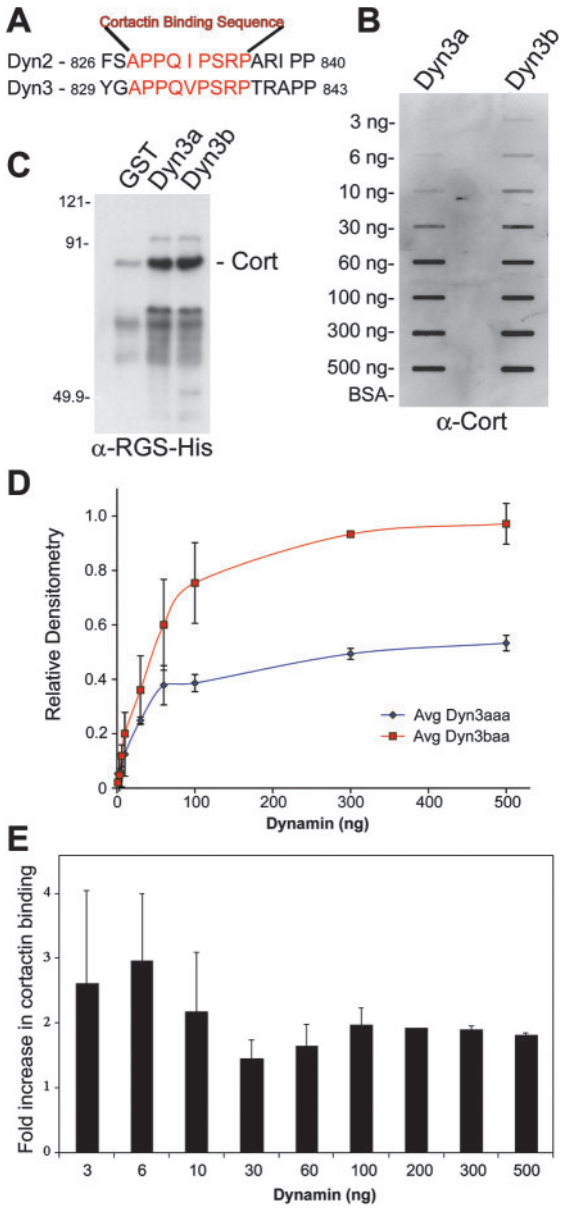

Fig. 5. Dyn3baa directly binds with a greater affinity than Dyn3aaa to the actin-associated protein cortactin. (A) Comparing the known cortactin binding site of Dyn2 with the correlative site in the Dyn3-PRD reveal that these sequences are almost identical. (B) Cortactin directly binds to both Dyn3aaa and Dyn3baa. GST alone failed to pull down the cortactin protein. (C) Dyn3aaa and Dyn3baa directly bind to cortactin in a blot overlay experiment using a range of recombinant Dyn3 protein amounts. (D) Binding curves representing densitometry measurements demonstrating the greater affinity for cortactin of Dyn3baa compared with Dyn3aaa. Results are normalized to the average maximum in each independent experiment and plotted on a scale of 0 to 1. Error bars represent the s.d. (E) Fold differences in binding of cortactin to Dyn3baa compared with Dyn3aaa. Results were from the average of three experiments and error bars represent the s.e.m.

Dyn3baa-cortactin interactions are needed to maintain dendritic filopodia

Cortactin has been previously shown to localize to dendritic spines (Hering and Sheng, 2003; Naisbitt et al., 1999), a finding we have confirmed using antibodies and exogenous cortactin-RFP expression (see Fig. S3 in supplementary material). In addition, we have previously demonstrated that disrupting the Dyn2-cortactin interaction through the expression of C-terminal deletion constructs results in the alteration of actin organization (McNiven et al., 2000). To test the physiological relevance of the Dyn3-cortactin interaction with respect to spine morphology, C-terminal truncation mutant constructs of the Dyn3 spliced forms (Dyn3ΔPRD) were engineered and expressed in cultured neurons (Fig. 6A). Neurons expressing Dyn3aaaΔPRD developed normally, with an extensive distribution of mushroom-shaped dendritic spines by 18DIV (Fig. 6B). These spines appeared to assemble synapses normally, based on the clustering of synapsin and PSD-95 (data not shown). Overall, the Dyn3aaaΔPRD signal was more diffuse, with fewer Dyn3aaa-GFP puncta than were observed for the wild-type GFP-tagged protein. By contrast, expression of the mutant Dyn3baaΔPRD did not induce filopodia but rather allowed the normal maturation program to proceed, with spines becoming the predominant dendritic protrusion by 18DIV (Fig. 6C). These spines assembled synapses normally, because both presynaptic and postsynaptic markers were observed at the tips of spines in Dyn3baaΔPRD-transfected neurons (data not shown). This was in marked contrast to mature neurons expressing wild-type Dyn3baa, which failed to exhibit clusters of PSD-95 at dendritic protrusions, indicating a reduction in neuronal synaptogenesis (Fig. 3B,D). These data suggest that the PRD of Dyn3baa is necessary for targeting this spliced variant to the appropriate machinery to modulate spinogenesis, potentially by binding to cortactin.

In reciprocal experiments designed to disrupt the Dyn3-cortactin interaction, neurons were co-transfected with a mutant cortactin missing the C-terminal SH3 domain (CortΔSH3) (Fig. 6D) and either wild-type Dyn3aaa or Dyn3baa. Initially, we tested whether CortΔSH3 affected neuronal development independent of Dyn3 expression. Synaptogenesis appeared to be unaffected by this mutant protein and it also continued to localize to dendritic spines, suggesting that the SH3 domain is not necessary for cortactin targeting (data not shown), a finding previously described by others (Hering and Sheng, 2003). There were no observed morphological changes in neurons expressing Dyn3aaa-GFP and CortΔSH3, with neurons exhibiting normal dendritic spines at 18DIV (Fig. 6E). By contrast, neurons expressing

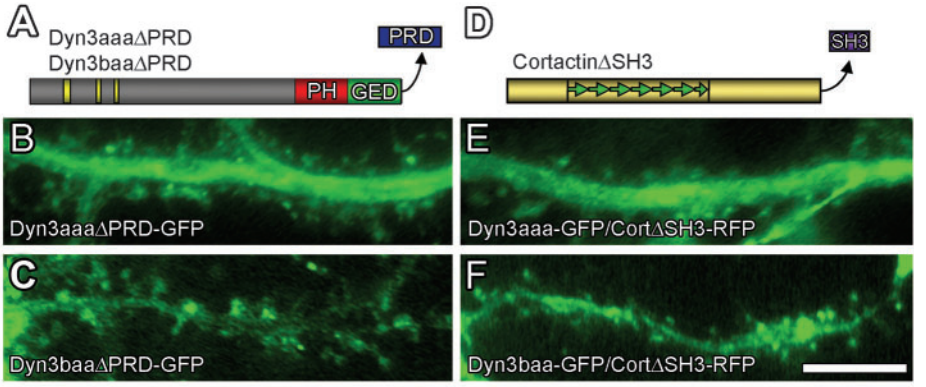

Fig. 6. Dyn3baa-induced filopodial outgrowth in mature neurons requires both the PRD of Dyn3 and full-length cortactin. (A) Dyn3aaa and Dyn3baa were truncated by 115 amino acids to remove the PRD and putative cortactin binding site. (B) Dyn3aaaΔPRD does not affect synaptogenesis. Neurons transfected with Dyn3aaaΔPRD-GFP show normal spine morphology at 18DIV. (C) Dyn3baaΔPRD does not induce filopodial outgrowth in mature neurons. Neurons transfected with Dyn3baaΔPRD-GFP exhibit normal spine morphology at 18DIV. (D) Cortactin was truncated by 73 amino acids, removing the SH3 domain and putative dynamin binding site. (E) Neurons co-transfected with Dyn3aaa and CortΔSH3-RFP display no morphological defects in mature spine development. (F) Dyn3baa requires full-length cortactin to cause filopodial outgrowth in mature neurons. Neurons co-transfected with Dyn3baa-GFP and CortΔSH3-RFP exhibit normal spine morphology at 18DIV, unlike neurons singly transfected with Dyn3baa-GFP. Scale bar, 5 μm.

both Dyn3baa-GFP and CortΔSH3 no longer displayed numerous filopodia at 18DIV (Fig. 6F), suggesting that the Dyn3baa-induced increase in filopodia is dependent upon binding to cortactin. Interestingly, although the immature filopodia normally induced by Dyn3baa were lost, Dyn3baa-GFP still trafficked to dendritic spines in the presence of CortΔSH3. This suggests that Dyn3baa can target to dendritic protrusions independent of cortactin, but, in order to function during filopodial induction, it must be recruited to actin filaments by cortactin.

Dyn3baa transcription is enhanced selectively during neuronal spinogenesis in vitro and in situ

The data described above suggest that increased levels of Dyn3baa might stimulate the production of filopodia on neurons (an event that normally occurs during development) but also maintains these filopodia in older neurons when filopodia are usually replaced by dendritic spines. Therefore, in transfected neurons, a sustained increase in Dyn3baa expression during maturation could cause a filopodium-dominated immature stage to persist, blocking the maturation of filopodia into spines. To explore the possibility that the neuron regulates the relative levels of endogenous Dyn3 spliceoforms, RNA was collected from cultured neurons at various stages of development for use in RT-PCR experiments.

Dyn3aaa mRNA levels were relatively stable between 1DIV and 21DIV, with a slight decrease in transcript copy number during synaptogenesis (7-14DIV) that was recovered by 21DIV (Fig. 7A). By contrast, Dyn3baa was barely detectable at the earlier stages of neuronal development, when neurites were forming and general polarity is established, but was substantially upregulated between 7DIV and 14DIV (Fig. 7A), the general timeframe for filopodium generation, synaptogenesis and a filopodium-to-spine transition (Jontes and Smith, 2000). By 14-21DIV, the ratio between the Dyn3aaa and Dyn3baa messages was roughly 1:1 but, in adult rat brains, there was a severalfold increase in the levels of Dyn3aaa over Dyn3baa. This suggested that, in the adult, either Dyn3aaa is upregulated with respect to Dyn3baa or the production of Dyn3baa is decreased with respect to Dyn3aaa after the critical time of synaptogenesis and filopodium/spine formation, possibly attenuating filopodium production in the adult neuron through a dilution of the Dyn3baa spliceoforms by the Dyn3aaa spliceoforms. To demonstrate equal transcript-copy-number loading in each PCR reaction, primers recognizing

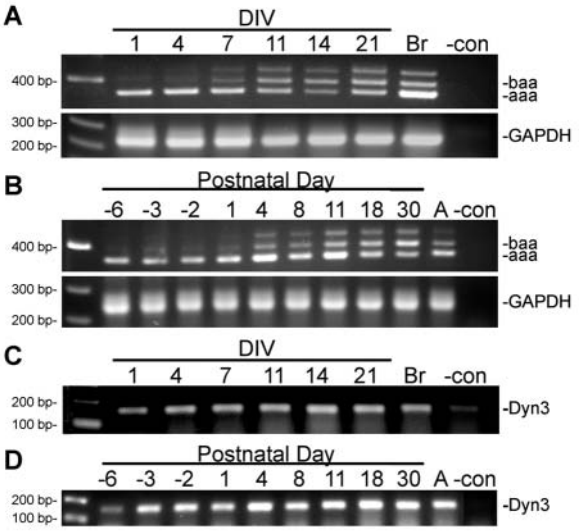

Fig. 7. Dyn3 transcripts are differentially regulated during neuronal development. (A) Isolated hippocampal neurons: primers flanking a 30-nucleotide spliced insert in *Dyn3* were used in RT-PCR reactions to assess the relative levels of *Dyn3aaa* and *Dyn3baa* in maturing cultured neurons at each age as labeled ('DIV' means 'days in vitro'). The *Dyn3aaa* product is 370 bp, whereas the *Dyn3baa* product is 400 bp. The PCR product at 430 bp is an RT-PCR artefact representing a heteroduplex of strands from each spliceoform. GAPDH RT-PCR demonstrates the use of equal amounts of template in each reaction. MW, molecular weight markers; Br, brain; –con, negative control. (B) Identical RT-PCR reactions were prepared using template derived from whole rat hippocampus at various developmental stages as listed above (P, postnatal day). GAPDH RT-PCR provides evidence for equal transcript copy number in the loading of template for each reaction. (C) RT-PCR using the cultured neuron template set and primers designed to exhibit total levels of all *Dyn3* transcripts. (D) RT-PCR using the whole hippocampi template set and primers designed to exhibit total levels of all *Dyn3* transcripts.

GAPDH were also used as a control (Fig. 7A). As an additional control, we also used primers to amplify a fragment of Dyn3 that is present in all known spliced variants (Cao et al., 1998). In this reaction, there was little difference in overall dynamin levels after 1DIV (Fig. 7C), suggesting that the tight regulation observed for Dyn3baa might be unique to this spliceoform and not a global phenomenon for other spliced variants.

A third band was observed in most of our reactions using these primers. In order to assess whether or not this band represented an additional Dyn3 spliced variant, we attempted to clone this fragment using a range of strategies or to amplify additional spliced variants using this band as template. In all cases, a unique fragment was not isolated nor amplified but, rather, Dyn3aaa and Dyn3baa fragments were consistently retrieved (data not shown). This led us to believe that the higher band at 430 bp is an artefact of the RT-PCR, with a heteroduplex forming between one strand from each of Dyn3aaa and Dyn3baa. This technical artefact has been well documented in other studies using RT-PCR to examine spliced variants (Zacharias et al., 1994).

To test whether the altered expression of the Dyn3baa form occurs in neurons in situ (in addition to in vitro), we isolated the hippocampus from rats at various stages of development and completed identical experiments to those described above. Interestingly, similar patterns of Dyn3 spliceoform expression were observed from whole hippocampus, with Dyn3aaa levels appearing to be unchanged throughout development, whereas Dyn3baa was dramatically upregulated at P4, the equivalent time as was observed in culture (Fig. 7B). Again, GAPDH levels were assessed at each time point, demonstrating an equal loading of transcript copy numbers for each reaction (Fig. 7B). Dyn3baa levels were maintained at an elevated level through P30 compared with Dyn3aaa but, again, in the adult, Dyn3aaa was the predominant spliceoform. As with the cultures, we also amplified all Dyn3 spliced variants and again saw little difference in overall Dyn3 levels after embryonic day 15, suggesting that the tight regulation of Dyn3baa might be unique to this spliceoform (Fig. 7D). In conclusion, there is a striking correlation between levels of endogenous Dyn3baa expression and filopodial growth in both cultured neurons and intact hippocampi that is consistent with a specific role for the Dyn3baa spliceoform in dendritic spine morphogenesis.

Discussion

In this study, we demonstrate a new and important function for the dynamin family of proteins, specifically a role for a distinct Dyn3 spliceoform (Dyn3baa) in the regulation of dendritic spine development and filopodium induction. When expressed in developing hippocampal neurons in culture, Dyn3baa localizes to and induces the formation of long filopodium-like immature spines. Exogenous expression of this Dyn3 form in epithelial cells also leads to the formation of numerous filopodia. Interestingly, a mutant form of this dynamin variant Dyn3baa(K44A) not only prevents filopodium formation in mature neurons and epithelial cells but also inhibits the normal formation of these structures in immature neurons. Instead, 11DIV neurons expressing Dyn3baa(K44A) produce morphologically mature spines, a characteristic of older (18-21DIV) neurons. Importantly, Dyn3baa binds with a 200% greater affinity to cortactin than does Dyn3aaa, an interaction mediated by the tails of these proteins. When the tail-to-tail interaction between Dyn3baa and cortactin is perturbed through the expression of truncation mutants, Dyn3baa can no longer mediate and sustain filopodial outgrowth in mature neurons. Last, although Dyn3aaa is constitutively expressed in neurons, a marked upregulation of *Dyn3baa* mRNA was observed in both cultured cells and whole hippocampi during the period of rapid synaptogenesis and spinogenesis, suggesting that the temporal expression of Dyn3 spliceoforms plays an important role during development. These results represent the first demonstration of a cooperative role for Dyn3 and cortactin in neuronal morphological remodeling, as well as additional evidence implicating the dynamin family of large GTPases in actin-dependent processes.

Dyn3, filopodia and actin

It has become clear that actin dynamics are important during the development and function of dendritic spines (Matus, 2000). Actin filaments are organized into a meshwork within both the head and spine neck, often with parallel actin bundles in the spine neck extending the barbed ends toward the spine head, with an extensive branching of those filaments within the head (Hirokawa, 1989; Landis and Reese, 1983). In addition, the actin cytoskeleton within the spines intimately associates with lipid microdomains, modulating the stability of the associating filaments (Itoh et al., 2002). This actin-membrane interplay was shown to be significant, because depletion of lipid rafts in cultured hippocampal neurons led to an overall decrease in spine density, implicating the membrane-cytoskeleton interaction as an integral modulator of spine development (Hering et al., 2003).

Despite these advances, few studies have identified protein links between actin and membranes during neuronal development. The dynamin family of GTPases is an attractive candidate as this link, because the association between dynamin and the membrane is well established and the number of studies implicating an interplay between dynamin and the actin cytoskeleton is steadily expanding (Orth and McNiven, 2003). Several groups have demonstrated a role for dynamin in the propulsion of vesicle comets (Lee and De Camilli, 2002; Orth et al., 2002) and in actin polymerization directly (Schafer et al., 2002). In previous work, enhanced expression of numerous actin-associated proteins, including debrin (Hayashi and Shirao, 1999), spinophilin/neurabin (Feng et al., 2000) and SPAR (Pak et al., 2001), have led to morphological changes in spines and filopodia. These studies, in conjunction with our own, underline the importance of the actin cytoskeleton and the proteins that modify it during normal filopodium and spine development.

An interesting finding of this study is the fact that two closely related Dyn3 forms mediate distinct spine morphologies when expressed in neurons. Alternative splicing in the dynamin family of mechanoenzymes is extremely important in determining the functional or localization behavior of each particular dynamin isoform. Dyn2 currently has four known spliced variants, with one particular spliceoform enriching at the Golgi and clathrin-coated pits, whereas another maintains a more cortical localization, associating with many endocytic structures (Cao et al., 1998). These two forms differ by only four amino acids, which reside

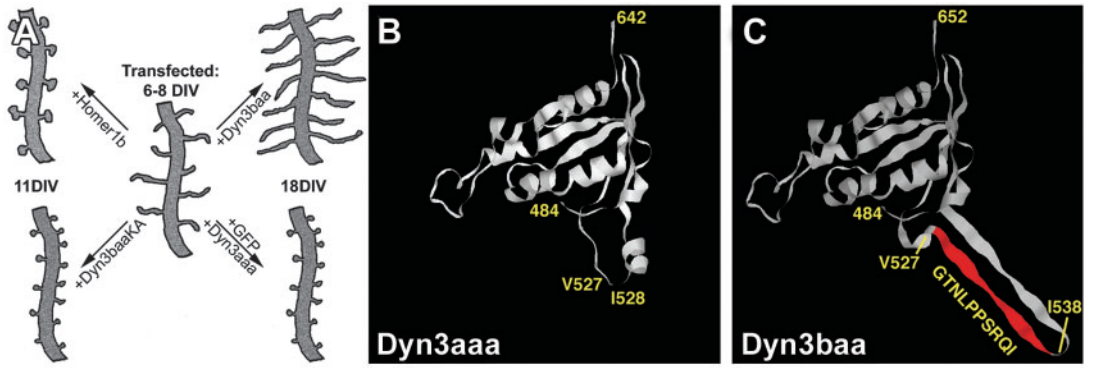

Fig. 8. Dyn3 interacts with PSD proteins to regulate dendritic spine maturation. (A) During synaptogenesis and early development, enhancing the expression of one of two PSD binding partners can lead to opposite dendritic spine phenotypes. Expression of Homer causes a supermaturation of spines, with these protrusions becoming larger and fully functional at an immature stage [11DIV (Sala et al., 2001)]. Conversely, expression of Dyn3baa inhibits the neuron from maturing and assembling spine synapses, leaving the cell in an immature state into the later stages of development (18DIV). An overabundance of another Dyn3 spliced variant (Dyn3aaa) or the GTPase-deficient Dyn3baa (Dyn3baaKA) has little effect on the normal spine developmental program; filopodia are eventually replaced by mushroom-shaped spines. (B,C) Theoretical modeling of Dyn3aaa (B) and Dyn3baa (C) of 100 amino acids around the PH domain based on the solved structure of Rac. Proline and charged residues in the insert [red in Dyn3baa (C)] might give rise to a protruding turned region extending away from the compact structure of the PH domain, as seen for Dyn3aaa in (B).

at precisely the same location in the molecule as the ten-amino-acid insert that differentiates Dyn3aaa and Dyn3baa. In addition, only particular spliceoforms of Dyn2 are involved in the modulation and maintenance of the centrosome (Thompson et al., 2004), another example of splicing leading to functional differences. Thus, important information for targeting and function are contained in these spliced areas, regardless of the identity between other domains between different spliceoforms.

In these studies, we provide additional evidence demonstrating a biochemical difference in binding affinity between Dyn3aaa and Dyn3baa (Fig. 5C), possibly owing to a conformational change in the two proteins induced by the ten-amino-acid insert, as our modeling suggests, despite the identity between the PRDs of Dyn3aaa and Dyn3baa. This slight modification in primary structure could induce a variation in the Dyn3baa three-dimensional conformation, optimally exposing surface epitopes and protein-protein interaction sites within the PRD. Because cortactin binds dynamin through an SH3-PRD interaction, folding differences that alter accessibility to the PRD might alter binding affinity. Molecular modeling using SWISS-MODEL of 100 amino acids around the PH domain of Dyn3, including the ten-amino-acid insert of Dyn3baa, was performed based on the solved crystal structure of the Rac PH domain (Hirshberg et al., 1997). The RasMac program allowed visualization of the theoretical structural differences caused by the ten-amino-acid insert in the Dyn3baa spliceoform (Fig. 8B,C). The modeling suggests that the combination of prolines and charged residues might promote the formation of a pronounced turn region extended away from the compact structure adjacent to the PH domain. Based on three-dimensional cryoelectron micrograph reconstructions of dynamin crystals (Zhang and Hinshaw, 2001), it is possible that any structural changes to the region around the PH domain could alter the interactions between multiple molecules of the ‘stalk’ region of dynamin oligomers and affect the way in which the PRD tail protrudes from the polymer. This, in turn, might affect binding properties with cortactin. We intend to explore this possibility using structural studies.

Dyn3, cortactin and spine formation

The pronounced interaction between the specific Dyn3 spliceoform (Dyn3baa) and cortactin defined above by in vitro binding experiments are consistent with the in vivo studies of Fig. 6, demonstrating that an immature neuronal phenotype in mature neurons is induced upon the disruption of the complex through expression of either Dyn3baaΔPRD or CortΔSH3.

Cortactin was originally identified as a cytoskeleton-interacting protein and substrate of Src (Wu and Parsons, 1993) and was recently linked to endocytosis (Cao et al., 2003). The cortactin protein bundles actin when it is dephosphorylated but, upon phosphorylation by Src, it exhibits reduced actin-cross-linking abilities (Huang et al., 1997). More recently, studies have demonstrated that cortactin might also function in cell migration owing to its dynamic and responsive relocalization to the cortex and actin-rich ruffles upon stimulation with growth factors (Krueger et al., 2003; McNiven et al., 2000). These examples emphasize the importance of cortactin-modulated actin dynamics, a concept that has since been applied to the neuronal actin cytoskeleton. Indeed, cortactin has been observed in the tips of ruffling growth cones, along with both CortBP1 (Du et al., 1998) and dynamin (N.W.G. and M.A.M., unpublished). In addition, cortactin localizes to dendritic spines, where it can interact with the scaffolding molecule Shank (Hering and Sheng, 2003; Naisbitt et al., 1999). This was a significant discovery, because it provides a link between the complex PSD network and the actin cytoskeleton, presumably the anchor for this receptor-containing complex. Our data demonstrating a role for Dyn3baa and cortactin in the morphological regulation of dendritic spines are consistent with this prediction, because the overexpression of Dyn3baa could change the properties of either the actin within the dendritic protrusion or the cortactin bundles themselves, and diminish the ability of these cytoskeletal structures to bind to the PSD complex.

Interestingly, both the GTPase activity of Dyn3baa and the PRD domain are necessary to initiate the production of filopodia that eventually develop into mature spines. Overexpression of Dyn3baa results in filopodia being abundantly present at 18DIV when spines are usually the

predominant dendritic structure (Fig. 1). When mutant Dyn3baa lacking the PRD is overexpressed, there is no phenotype, suggesting that this protein is rendered nonfunctional and irrelevant from the standpoint of spine homeostasis (owing to a lack of proper targeting) and that the neuron can thus develop normally. Improper targeting induced by the removal of the dynamin PRD has been exploited in a number of studies to demonstrate a loss-of function for dynamin (Orth et al., 2002). When Dyn3baa(K44A) (lacking GTPase activity) is expressed, there is no 'filopodial phenotype' (i.e. normal spines develop). Interestingly, with the expression of Dyn3baa(K44A), there is in fact a reduction in overall filopodial density, with more mature protrusions present instead. This suggests that Dyn3baa does indeed perform a direct role in dendritic filopodial growth because, when the GTPase-dead mutant is expressed, it acts as a dominant-negative mutant, incorporating into Dyn3baa-containing tetramers and disrupting the functionality of the complex. Without functional Dyn3baa tetramers, the modulation of dendritic protrusion growth is shifted away from actin-rich filopodia, thus causing the appearance of mature-looking protrusions at an earlier age. With dynamin classified as a mechanoenzyme, it follows that GTPase activity can cause a conformational shift in the structure of the dynamin oligomeric complex, a necessary task to sever vesicles during endocytosis (Danino et al., 2004). This same conformational shift could change the way that dynamin interacts with other proteins or performs tasks related to actin regulation through these interacting proteins (like cortactin). Precedence for this comes from studies demonstrating a reduction of actin-based vesicle motility in cells expressing mutant Dyn2 (Lee and De Camilli, 2002; Orth et al., 2002), a reduction of in vivo actin dynamics at the periphery of motile cells (Schafer et al., 2002) and a reduction of actin turnover at podosomes (Ochoa et al., 2000). Thus, links between the GTPase activity of dynamin isoforms, the consequences of GTPase-deficient mutants on actin-based structures (such as dendritic filopodia and spines) and actin binding proteins (like cortactin) are well established in the literature, leading to the conclusions in this report.

Transcriptional regulation of Dyn3 spliceoforms

To explore the mechanisms mediating the filopodial induction observed by the overexpression of Dyn3baa, we first examined the expression of Dyn3 spliceoform mRNA to determine whether there was a difference in expression between Dyn3aaa and Dyn3baa as neurons matured. A hypothesis to explain our original results assumed that the constitutive increase and transient expression of Dyn3baa by the powerful cytomegalovirus (CMV) promoter could be a cause for the lack of morphological maturation by the neuron, because any regulation of Dyn3 spliceoform expression would be eliminated. Therefore, a sustained excess of Dyn3baa could lead to a maintenance of dendritic filopodia (Fig. 8A). In a similar fashion, the Dyn3-binding protein Homer also influences the maturation process of the neuron, because early enhanced expression of this protein causes a rapid maturation in neurons, with younger neurons becoming morphologically similar to fully mature neurons (Sala et al., 2001). Thus, although Homer is normally upregulated during the late stages of synaptogenesis and postsynaptic formation (Brakeman et al., 1997), temporal manipulation of its expression causing the neuron to produce more Homer at an earlier time point can alter synaptic functionality. We explored a similar concept in our model system, because RT-PCR results suggested that, although Dyn3aaa was constitutively produced, *Dyn3baa* message increased rapidly in parallel with the increases in filopodium production. This was followed by a slight reduction in *Dyn3baa* transcript production in adulthood, when filopodium outgrowth is reduced (Fig. 8A). Therefore, a temporally regulated splicing of the *Dyn3* transcript to produce the Dyn3baa spliceoform at a particular stage in development might facilitate a role in filopodium production. In turn, a subsequent reduction of this message later in development could reduce filopodium formation. The persistent overexpression of exogenous Dyn3baa might disrupt this delicate balance of Dyn3 spliceoform control, producing the observed phenotypes in this study. Because these changes in spliceoform transcript levels are observed not only in cultured neurons, but also from whole hippocampus, it is likely that a regulation of Dyn3 splicing plays an important role during in vivo synaptogenesis.

This study provides novel evidence indicating a functional relevance for alternative splicing within the *Dyn3* transcript and subsequent implications during synaptogenesis. With 13 putative Dyn3 spliceoforms (Cao et al., 1998), many undiscovered functional possibilities remain for Dyn3 in the neuron.

We thank P. McPherson for the generous gift of reagents, H. Cao, J. Kim and J. D. Orth for technical assistance, W. Hu for help with statistics, M. Ramirez-Alvarado for useful discussions, and the McNiven lab for various assistance regarding this study.

References

Brakeman, P. R., Lanahan, A. A., O'Brien, R., Roche, K., Barnes, C. A., Huganir, R. L. and Worley, P. F. (1997). Homer: a protein that selectively binds metabotropic glutamate receptors. *Nature* **386**, 284-288.

Cao, H., Garcia, F. and McNiven, M. A. (1998). Differential distribution of dynamin isoforms in mammalian cells. *Mol. Biol. Cell* **9**, 2595-2609.

Cao, H., Orth, J. D., Chen, J., Weller, S. G., Heuser, J. E. and McNiven, M. A. (2003). Cortactin is a component of clathrin-coated pits and participates in receptor-mediated endocytosis. *Mol. Cell. Biol.* **23**, 2162-2170.

Cook, T. A., Urrutia, R. and McNiven, M. A. (1994). Identification of dynamin **2**, an isoform ubiquitously expressed in rat tissues. *Proc. Natl. Acad. Sci. USA* **91**, 644-648.

Cook, T., Mesa, K. and Urrutia, R. (1996). Three dynamin-encoding genes are differently expressed in developing rat brain. *J. Neurochem.* **67**, 927-931.

Dailey, M. E. and Smith, S. J. (1996). The dynamics of dendritic structure in developing hippocampal slices. *J. Neurosci.* **16**, 2983-2994.

Damke, H., Baba, T., Warnock, D. E. and Schmid, S. L. (1994). Induction of mutant dynamin specifically blocks endocytic coated vesicle formation. *J. Cell Biol.* **127**, 915-934.

Danino, D., Moon, K. H. and Hinshaw, J. E. (2004). Rapid constriction of lipid bilayers by the mechanochemical enzyme dynamin. *J. Struct. Biol.* **147**, 259-267.

Du, Y., Weed, S. A., Xiong, W. C., Marshall, T. D. and Parsons, J. T. (1998). Identification of a novel cortactin SH3 domain-binding protein and its localization to growth cones of cultured neurons. *Mol. Cell. Biol.* **18**, 5838-5851.

El-Husseini, A. E., Schnell, E., Chetkovich, D. M., Nicoll, R. A. and Bredt, D. S. (2000). PSD-95 involvement in maturation of excitatory synapses. *Science* **290**, 1364-1368.

Feng, J., Yan, Z., Ferreira, A., Tomizawa, K., Liauw, J. A., Zhuo, M., Allen, P. B., Ouimet, C. C. and Greengard, P. (2000). Spinophilin regulates the formation and function of dendritic spines. *Proc. Natl. Acad. Sci. USA* **97**, 9287-9292.

Fiala, J. C., Feinberg, M., Popov, V. and Harris, K. M. (1998). Synaptogenesis via dendritic filopodia in developing hippocampal area CA1. *J. Neurosci*. **18**, 8900-8911.

Gray, N. W., Fourgeaud, L., Huang, B., Chen, J., Cao, H., Oswald, B. J., Hemar, A. and McNiven, M. A. (2003). Dynamin 3 is a component of the postsynapse, where it interacts with mGluR5 and Homer. *Curr. Biol*. **13**, 510-515.

Guex, N. and Peitsch, M. C. (1997). SWISS-MODEL and the Swiss-PdbViewer: an environment for comparative protein modeling. *Electrophoresis* **18**, 2714-2723.

Hayashi, K. and Shirao, T. (1999). Change in the shape of dendritic spines caused by overexpression of drebrin in cultured cortical neurons. *J. Neurosci*. **19**, 3918-3925.

Hering, H. and Sheng, M. (2001). Dendritic spines: structure, dynamics and regulation. *Nat. Rev. Neurosci.* **2**, 880-888.

Hering, H. and Sheng, M. (2003). Activity-dependent redistribution and essential role of cortactin in dendritic spine morphogenesis. *J. Neurosci*. **23**, 11759-11769.

Hering, H., Lin, C. C. and Sheng, M. (2003). Lipid rafts in the maintenance of synapses, dendritic spines, and surface AMPA receptor stability. *J. Neurosci*. **23**, 3262-3271.

Hirokawa, N. (1989). The arrangement of actin filaments in the postsynaptic cytoplasm of the cerebellar cortex revealed by quick-freeze deep-etch electron microscopy. *Neurosci. Res*. **6**, 269-275.

Hirshberg, M., Stockley, R. W., Dodson, G. and Webb, M. R. (1997). The crystal structure of human rac1, a member of the Rho-family complexed with a GTP analogue. *Nat. Struct. Biol*. **4**, 147-152.

Huang, C., Ni, Y., Wang, T., Gao, Y., Haudenschild, C. C. and Zhan, X. (1997). Down-regulation of the filamentous actin cross-linking activity of cortactin by Src-mediated tyrosine phosphorylation. *J. Biol. Chem*. **272**, 13911-13915.

Itoh, K., Sakakibara, M., Yamasaki, S., Takeuchi, A., Arase, H., Miyazaki, M., Nakajima, N., Okada, M. and Saito, T. (2002). Cutting edge: negative regulation of immune synapse formation by anchoring lipid raft to cytoskeleton through Cbp-EBP50-ERM assembly. *J. Immunol*. **168**, 541-544.

Jontes, J. D. and Smith, S. J. (2000). Filopodia, spines, and the generation of synaptic diversity. *Neuron* **27**, 11-14.

Krueger, E. W., Orth, J. D., Cao, H. and McNiven, M. A. (2003). A dynamin-cortactin-Arp2/3 complex mediates actin reorganization in growth factor-stimulated cells. *Mol. Biol. Cell* **14**, 1085-1096.

Landis, D. M. and Reese, T. S. (1983). Cytoplasmic organization in cerebellar dendritic spines. *J. Cell Biol.* **97**, 1169-1178.

Lee, E. and de Camilli, P. (2002). Dynamin at actin tails. *Proc. Natl. Acad. Sci. USA* **99**, 161-166.

Matus, A. (2000). Actin-based plasticity in dendritic spines. *Science* **290**, 754-758.

McNiven, M. A., Kim, L., Krueger, E. W., Orth, J. D., Cao, H. and Wong, T. W. (2000). Regulated interactions between dynamin and the actin-binding protein cortactin modulate cell shape. *J. Cell Biol.* **151**, 187-198.

Naisbitt, S., Kim, E., Tu, J. C., Xiao, B., Sala, C., Valtschanoff, J., Weinberg, R. J., Worley, P. F. and Sheng, M. (1999). Shank, a novel family of postsynaptic density proteins that binds to the NMDA receptor/PSD-95/GKAP complex and cortactin. *Neuron* **23**, 569-582.

Nakata, T., Iwamoto, A., Noda, Y., Takemura, R., Yoshikura, H. and Hirokawa, N. (1991). Predominant and developmentally regulated expression of dynamin in neurons. *Neuron* **7**, 461-469.

Nakata, T., Takemura, R. and Hirokawa, N. (1993). A novel member of the dynamin family of GTP-binding proteins is expressed specifically in the testis. *J. Cell Sci.* **105**, 1-5.

Notredame, C., Higgins, D. G. and Heringa, J. (2000). T-Coffee: a novel method for fast and accurate multiple sequence alignment. *J. Mol. Biol.* **302**, 205-217.

Ochoa, G. C., Slepnev, V. I., Neff, L., Ringstad, N., Takei, K., Daniell, L., Kim, W., Cao, H., McNiven, M., Baron, R. et al. (2000). A functional link between dynamin and the actin cytoskeleton at podosomes. *J. Cell Biol.* **150**, 377-390.

Orth, J. D. and McNiven, M. A. (2003). Dynamin at the actin-membrane interface. *Curr. Opin. Cell Biol.* **15**, 31-39.

Orth, J. D., Krueger, E. W., Cao, H. and McNiven, M. A. (2002). The large GTPase dynamin regulates actin comet formation and movement in living cells. *Proc. Natl. Acad. Sci. USA* **99**, 167-172.

Pak, D. T., Yang, S., Rudolph-Correia, S., Kim, E. and Sheng, M. (2001). Regulation of dendritic spine morphology by SPAR, a PSD-95-associated RapGAP. *Neuron* **31**, 289-303.

Papa, M., Bundman, M. C., Greenberger, V. and Segal, M. (1995). Morphological analysis of dendritic spine development in primary cultures of hippocampal neurons. *J. Neurosci*. **15**, 1-11.

Peitsch, M. C. (1995). Protein modeling by E-mail. *Biotechnology* **13**, 658-660.

Poirot, O., Suhre, K., Abergel, C., O'Toole, E. and Notredame, C. (2004). 3DCoffee: a web server for mixing sequences and structure into multiple sequence alignments. *Nucleic Acids Res.* **32**, W39-W40.

Sala, C., Piech, V., Wilson, N. R., Passafaro, M., Liu, G. and Sheng, M. (2001). Regulation of dendritic spine morphology and synaptic function by Shank and Homer. *Neuron* **31**, 115-130.

Schafer, D. A. (2002). Coupling actin dynamics and membrane dynamics during endocytosis. *Curr. Opin. Cell Biol.* **14**, 76-81.

Schafer, D. A., Weed, S. A., Binns, D., Karginov, A. V. and Cooper, J. A. (2002). Dynamin 2 and cortactin regulate actin assembly and filament organization. *Curr. Biol*. **12**, 1852-1857.

Schwede, T., Kopp, J., Guex, N. and Peitsch, M. C. (2003). SWISS-MODEL: an automated protein homology-modeling server. *Nucleic Acids Res.* **31**, 3381-3385.

Shupliakov, O., Low, P., Grabs, D., Gad, H., Chen, H., David, C., Takei, K., de Camilli, P. and Brodin, L. (1997). Synaptic vesicle endocytosis impaired by disruption of dynamin-SH3 domain interactions. *Science* **276**, 259-263.

Sontag, J.-M., Fykse, E. M., Ushkaryov, Y., Liu, J.-P., Robinson, P. J. and Sudhof, T. C. (1994). Differential expression and regulation of multiple dynamins. *J. Biol. Chem*. **269**, 4547-4554.

Sorra, K. E. and Harris, K. M. (2000). Overview on the structure, composition, function, development, and plasticity of hippocampal dendritic spines. *Hippocampus* **10**, 501-511.

Takei, K., Mundigl, O., Daniell, L. and de Camilli, P. (1996). The synaptic vesicle cycle: a single vesicle budding step involving clathrin and dynamin. *J. Cell Biol.* **133**, 1237-1250.

Thompson, H. M., Cao, H., Chen, J., Euteneuer, U. and McNiven, M. A. (2004). Dynamin 2 binds gamma-tubulin and participates in centrosome cohesion. *Nat. Cell Biol.* **6**, 335-342.

Wu, H. and Parsons, J. T. (1993). Cortactin, an 80/85-kiloDalton pp60^{Src} substrate, is a filamentous actin-binding protein enriched in the cell cortex. *J. Cell Biol.* **120**, 1417-1426.

Zacharias, D. A., Garamszegi, N. and Strehler, E. E. (1994). Characterization of persistent artifacts resulting from RT-PCR of alternatively spliced mRNAs. *BioTechniques* **17**, 652-655.

Zhang, P. and Hinshaw, J. E. (2001). Three-dimensional reconstruction of dynamin in the constricted state. *Nat. Cell Biol.* **3**, 922-926.

Ziv, N. E. and Smith, S. J. (1996). Evidence for a role of dendritic filopodia in synaptogenesis and spine formation. *Neuron* **17**, 91-102.